1990 SCA CONFERENCE PAPER NUMBER 9006

NIPER Paper EPR/OP.90/5

INVESTIGATION OF CYCLE DEPENDENT CENTRIFUGE CAPILLARY PRESSURE AND WETTABILITY INDEX BEHAVIOR FOR WATER-WET HIGH PERMEABILITY SANDSTONES

PAPER SCA 9006

By

Matt Honarpour and Dan Maloney
IITRI/National Institute for Petroleum and Energy Research

Shogo Suzuki
Japan Petroleum Exploration CO., LTD.

and Liviu Tomutsa
IITRI/National Institute for Petroleum and Energy Research

For presentation at the
Fourth Annual SCA Technical Conference
to be held in Dallas, TX on August 15-16, 1990

IIT Research Institute
NATIONAL INSTITUTE FOR PETROLEUM AND ENERGY RESEARCH
P. O. Box 2128
Bartlesville, Oklahoma 74005
(918) 336-2400

INVESTIGATION OF CYCLE DEPENDENT CENTRIFUGE CAPILLARY PRESSURE AND WETTABILITY INDEX BEHAVIOR FOR WATER-WET HIGH-PERMEABILITY SANDSTONES

By
Matt Honarpour and Dan Maloney
IITRI/National Institute for Petroleum and Energy Research

Shogo Suzuki
Japan Petroleum Exploration CO., LTD.

and Liviu Tomutsa
IITRI/National Institute for Petroleum and Energy Research

ABSTRACT

A laboratory investigation was conducted to examine cycle dependent centrifuge capillary pressure and wettability index behavior for water-wet high-permeability sandstones. Fired plugs of Bentheimer and two Berea sandstones of different permeabilities were used for this investigation. The Bentheimer and Berea samples were physically and chemically similar except for their pore throat diameter distributions.

Plugs 3.8 cm in diameter by 3.8 cm long jacketed circumferentially with Teflon tape were tested with inert brine and oil in a high-speed centrifuge that induced capillary pressures to 207 kPa (30 psi). Experiments were conducted with multiple drainage/imbibition saturation cycles under varying conditions of maximum capillary pressure and equilibration time. CT scans, mercury injection porosimetry tests, and spontaneous imbibition tests were used as aids in evaluating the effects of pore geometry and pore size distribution on capillary pressure and wettability index.

Results showed that, for these plugs, the order of increasing permeability and increasing susceptibility to hysteresis was the same as the order of increasing median pore diameter. Hysteresis was evident in the results from each multiple-cycle capillary pressure experiment. The primary effect of cycle dependent hysteresis for these samples was a reduction in the wettability index with successive drainage and imbibition cycles. CT images showed that different fluid distributions resulted for rocks of different pore throat size and pore volume characteristics at similar capillary pressures. These fluid distributions were non-uniform except at high capillary pressures. Jacketing a high permeability Berea plug with Teflon tape did not stop brine imbibition from occurring around the plug margins. Finally, a centrifuge capillary pressure report form is presented to allow better documentation of parameters that may influence capillary pressure and wettability results.

INTRODUCTION

Capillary pressure information is used in a variety of petroleum engineering calculations. The accuracies of reservoir simulations are dependent on the quality of the data used. Accurate laboratory measurements of capillary pressure are important, as documented by Anderson (1987a, 1987b) and emphasized by Hawkins and Bouchard (1989).

Limited studies have been conducted to investigate capillary pressure/saturation hysteresis effects. Several studies have touched upon the question of the magnitudes and effects of hysteresis on centrifuge capillary pressure/saturation data, such as those by Harris and Morris (1965), Evrenos and Comer (1969) , Szabo (1970), Batycky et al. (1981), and Longeron et al. (1986). Others have investigated the influence of reservoir or experimental conditions on hysteresis such as the temperature studies of Sinnokrot et al. (1971) and Sanyal et al. (1973). Several studies have suggested that wettability and/or pore size distribution are responsible for capillary pressure/saturation hysteresis.

The purpose of this investigation was to examine the relationships among cycle dependent hysteresis in capillary pressure and wettability index measurements and pore throat size distributions for water-wet high-permeability sandstone rocks.

EXPERIMENTAL PROCEDURES

SAMPLE PREPARATION

Plug and rock samples were cut from blocks of Bentheimer and Berea sandstones. These sandstones were selected because of their homogeneous characteristics and were designated A (Bentheimer), B (high-permeability Berea), and C (intermediate-permeability Berea). Plugs of 3.8 cm diameter and length were cut for centrifuge capillary pressure tests. Plugs of 2.5 cm diameter and length were cut for mercury injection porosimetry tests. Additional samples of rock were obtained for X-ray diffraction (XRD) analysis. All samples were fired at 1,000° C to render clay minerals inert. Plugs for centrifuge capillary pressure tests were marked to establish permanent orientations.

MERCURY INTRUSION TESTS

Air permeabilities and porosities were measured on plugs of A, B, and C before they were characterized by mercury intrusion porosimetry. Volume and pressure measurements from tests in which mercury was forced into the rock pores at pressures from 3.45 kPa to 413.7 MPa (0.5 to 60,000 psia) were used to calculate pore throat diameters and size distributions.

AMOTT TESTS

Plugs of A, B, and C at residual saturation conditions were placed in brine-filled Amott cells. The volume of oil drained from each plug was measured over a 10-day period. Similar tests were conducted with plugs containing residual oil saturations that were placed in oil-filled Amott cells.

Two additional brine-saturated plugs of B and C were centrifuged in oil at 1,500 RPM for 24 hr to residual brine saturation conditions. The plugs were then transferred to brine filled containers which were placed in the rockholder. CT scans were taken of the rocks as they imbibed brine to monitor the imbibition process after 1 minute, 15 minutes, and 60 hours.

CENTRIFUGE CAPILLARY PRESSURE TESTS

Three sets of experiments were conducted during this investigation: high RPM, long-term tests using samples A and B; low RPM, long-term (first cycle) and short-term (second cycle) tests using samples B and C; and low RPM short-term tests using samples A, B and C. Each plug was wrapped circumferentially with Teflon tape and was marked to facilitate reorientation with respect to the axis of rotation within the centrifuge after transfer from one tube to another as a test progressed with a change in saturation direction or for reorientation after a CT scan. The jacket of Teflon tape was used in an effort to prevent radial fluid transfer and to minimize fluid loss from handling. The fluids used in this investigation consisted of a low-salinity brine (1% by weight NaCl in deionized water) and a low-viscosity isoparaffinic oil (Soltrol 100, Phillips Petroleum Co.). The low salinity was deemed appropriate since the plugs were fired to stabilize clay minerals. The fluids were characterized by viscosity, density, and interfacial tension (IFT) measurements. The first step in each centrifuge capillary pressure test was to saturate the plugs with brine using procedures recommended by Worthington (1978). Pore volumes were calculated from both gas expansion (Boyle's law) and weight-change methods.

A Beckman J-6M centrifuge was used for this work. The temperature within the centrifuge was maintained at 25° C during each test. Special centrifuge buckets and tubes were built to accommodate the 3.8 cm diameter by 3.8 cm long samples. The resulting buckets were too heavy to swing to a horizontal position at low centrifuge speeds, so mounts were designed to allow the buckets to be affixed horizontally at the start of a test before turning on the centrifuge. This provided the capability for these experiments to record displaced fluid volume measurements at centrifuge speeds from 200 to 4,000 RPM, corresponding to oil-water capillary pressures from about 0.97 to 200 kPa (0.14 to 29 psi) for drainage cycles and 1.31 to 263 kPa (0.19 to 38.1 psi) for imbibition cycles. A variable-intensity strobe was mounted within the centrifuge below the buckets. The strobe control circuitry was designed to freeze the apparent motion of any one of the four centrifuge buckets immediately upon activating the strobe. The intensity of the strobe light was adjusted from its highest level at slow speeds to a lower intensity at

high speeds according to the amount of light required to read the volumes in the tubes. Special care was taken when changing centrifuge speeds to prevent overshooting the target speed. Care was taken to balance the weights of the centrifuge buckets to prevent vibration. Nevertheless, the centrifuge had what appeared to be a resonating frequency around 600 RPM, at which speed excessive vibrations occurred. Care was taken to avoid measurements at rotational speeds close to 600 RPM and to quickly pass the 600 RPM speed when changing from lower to higher settings.

High RPM, Long-Term Tests--Long-duration, high RPM tests were conducted on plugs of A and B. The plugs were placed in drainage tubes under oil and were centrifuged at nine rotational speeds from 400 RPM to 4,000 RPM. Each speed was maintained for 48 hr before recording the final displaced brine volumes. After completing the first drainage cycle, the plugs were placed under brine in imbibition tubes. Measurements of displaced oil were recorded at centrifuge speeds and times similar to those from the drainage test. Tests continued with second drainage, second imbibition, and third drainage cycles.

Low RPM, Long- and Short-Term Tests--Plugs of B and C were used for long- and short-term tests. The long-term tests were conducted like the long-term, high RPM tests except that measurements were restricted to six centrifuge speeds from 200 to 1,500 RPM and that only a first imbibition and second drainage cycle followed the initial drainage cycle. The short-term tests were continued on the same plugs by recording measurements during second imbibition and third drainage cycles at similar rotational speeds but with equilibration times of only 1 hr rather than 48 hr.

Low RPM, Short-Term Tests--These tests were conducted on plugs of B and C for first drainage, first imbibition, and second drainage cycles with measurements recorded after 1 hr of rotation at each of six rotational speeds between 200 and 1,500 RPM.

Centrifuge/CT Scan Tests--Plugs B and C were used to evaluate fluid distributions during centrifuge capillary pressure measurements. The plugs were marked so that their orientations could be maintained throughout the centrifuge tests and so that each CT scan was of the same plane through the center of the plug from end to end. Plugs were placed in a vertical position in a 12.7-cm rockholder that was designed to minimize image artifacts due to effects unrelated to fluid saturations. CT scans were conducted using a third generation Siemens X-ray CT scanner using 125 kV and 460 mAs power settings.

After scanning the plugs in their dry condition, the plugs were saturated with brine. The brine was tagged with 10% KBr by weight to provide a high X-ray attenuation contrast between the oil and brine on CT scan images. Scans were taken of the brine-saturated plugs. Next, the plugs were placed in oil within

centrifuge drainage cells. The oil was 1.2 cP Soltrol 100, a refined isoparaffinic oil from Phillips Petroleum Company. The plugs were centrifuged under oil for 48 hr at 1,500 RPM. The 1,500 RPM rotational speed induced a capillary pressure of 49.6 kPa (7.2 psi) and was selected to provide a residual brine saturation similar to that which results from dynamic displacement during a linear coreflood test. Scans were taken of the plugs under residual brine saturation conditions. The plugs were then placed in imbibition cells under brine and were rotated in the centrifuge at 100 RPM for 48 hr. At the end of the 48-hr period, the centrifuge was shutdown. As soon as the centrifuge buckets stopped, the plugs were removed from the imbibition cells and were CT scanned. The plugs were returned to the imbibition cells and were replaced in the centrifuge within 10 minutes. Additional scans were taken in a similar manner after 48 hr at rotational speeds of 120, 130, 140, 150, 200, 300, 400, 800, 1,000, 1,200, and 1,500 RPM. Thereafter, the plugs were placed in drainage cells under oil. Scans were taken after 48 hr at rotational speeds of 100, 200, 300, 400, 800, 1,000, 1,200, and 1,500 RPM.

RESULTS

Samples A, B, and C were almost identical in mineralogy. Clay analysis XRD results for the three samples are shown in Fig. 1. Petrophysical properties and pore characteristics from routine core analysis and mercury porosimetry are presented in Table 1. Sample A had the highest permeability, followed by sample B and then C. Similarly, sample A had the largest median pore diameter, followed by B and then C. Clay mineral peaks on XRD results for the unfired samples of the rocks disappeared after firing, indicating a collapse of the layered crystalline structure of the clays. Quartz and feldspar grains were not significantly altered or shattered by firing; however, iron sulfides, siderite, and ferroan dolomite were converted to hematite, giving the rocks a reddish color. Calcium carbonate turns to calcium hydroxide in the presence of water in fired Berea rocks. When neutral pH brine is pumped through Berea that had been fired at high temperature, the pH of the effluent can be very basic, as reported by Shaw et al. (1989) . The pH of effluent from plugs B and C when neutral brine was pumped through the fired plugs was initially in the 10.5 to 11 range, where the pH of the effluent from plug A was neutral. Results from tests to characterize the fluids are shown in Table 2. Little difference was found between the interfacial tensions for oil (Soltrol 100) and the neutral or high pH brine.

MERCURY INTRUSION

Fig. 2, a plot of log specific differential intrusion volume versus pore diameter, provides information on the pore throat size distributions for the three samples. The plot shows the fairly narrow pore throat size distribution of sample A compared to the other two samples as well as the higher degree of microporosity exhibited by samples B and particularly C. The units for log differential intrusion volume on Fig. 2 are $cm^3/gram/\mu m$.

AMOTT TESTS

The plugs placed under brine in the Amott cells had undergone two sets of drainage and imbibition capillary pressure tests and were at residual water saturation conditions. After 10 days, plug A had imbibed a brine volume equal to 26 % of the pore volume, whereas B and C had imbibed 39 and 34 % respectively. The final brine saturations were 33, 56, and 58 % for plugs A, B and C. The plugs at residual oil saturation that were placed in oil did not imbibe any oil. These results show that the rocks had a much greater affinity for brine than oil.

Fig. 3 shows CT images at intervals of 1 minute, 15 minutes, and 60 hours of plugs B and C as they imbibed brine. The top of the plugs face toward the top of the page in the figure. Even though the plugs were initially at residual brine saturation conditions, they imbibed significant volumes of brine after only 1 minute of immersion in brine. The plugs imbibed brine from both radial and axial directions. After initially imbibing significant quantities of brine, the imbibition process slowed considerably as continuity of oil channels to the upper plug surface was disrupted. Even after a week, CT images of each rock showed a large area at high oil saturation surrounded by the imbibed brine. Reorienting the plugs did not cause any additional oil displacement or change in the shape and position of the trapped oil.

CENTRIFUGE CAPILLARY PRESSURE TESTS

Data from the centrifuge capillary pressure tests (displaced fluid volumes, centrifuge rotational speed, rotor radius for drainage, and imbibition) and rock and fluid characteristics were used to construct capillary pressure versus saturation curves and to calculate wettability indices. Most of the capillary pressure-saturation relationships were determined using both the Hassler-Brunner (1945) and Rajan (1986) methods, and all of the results were analyzed by the Rajan method. Wettability indices were calculated using the USBM technique (Donaldson and Lorenz, 1969). Wettability index results are shown in Table 3. Capillary pressure-saturation results from Hassler-Brunner and Rajan solutions were similar, and these similarities are reflected in the wettability index values.

High RPM, Long-Term Tests--Maximum capillary pressures developed during the high RPM, long-term tests were 200 kPa (29 psi) during drainage and 262 kPa (38 psi) during imbibition cycles. The first and second drainage cycles for plug A were nearly identical ,whereas the third imbibition curve shifted in the direction of higher water saturation for capillary pressures greater than about 14 kPa (2 psi), as shown in Fig. 4. The second imbibition curve shifted toward lower water saturations, with respect to the first imbibition curve. The negative wettability indices for the two sets of imbibition and drainage data, which suggest that the rock had a greater affinity for oil than water, are not consistent with the results from the Amott cell test and are thought to be a result of the high capillary pressures induced during the

imbibition cycles in combination with pore size distribution within the rock. When data for capillary pressures greater than 6 psi were ignored, the wettability indices for plug A were 0.5 and 0.4 for the two cycles. These values are more consistent with the behavior expected for plug A.

The drainage curves for plug B were all different although portions of the curves were similar for the three drainage cycles. The imbibition curves were almost identical, as shown in Fig. 5. The wettability indices indicated that the sample had a greater affinity for water than oil, which is compatible with the Amott test data. The high brine saturations at low capillary pressures that resulted during the imbibition cycles were also consistent with the Amott test results.

Low RPM, Long- and Short-Term Tests--Results from plugs B and C showed hysteresis in both drainage and imbibition cycles when the first imbibition, first and second drainage curves from the long-duration (48 hr/pt) tests were compared with the second imbibition and third drainage results from the short-duration (1hr/pt) tests. The shifts in the drainage curves appeared to be random, whereas the second imbibition cycle curves were offset from the first cycle curves in the direction of lower water saturation with more gentle curvature at capillary pressures up to about 21 kPa (3 psi), then converged with the first cycle curves as the residual oil saturation was approached.

Low RPM, Short-Term Tests--Low RPM, short-term capillary pressure-saturation curves and wettability indices were comparable with the those from low RPM, long- and short-term tests for samples B and C. Plug B curves and wettabilities for this test were also similar to those resulting from the high RPM, long-term test. Plug A results from this test were much different than those for the same plug from the high RPM test. It appears from the plug A data that a significant portion of the water imbibed during the start of the imbibition cycle was spontaneous, yielding a very abrupt imbibition curve.

A sensitivity analysis performed on the data indicated that a 5% error in pore volume or fluid density measurement did not affect the wettability indices significantly.

Centrifuge/CT Scans--CT scans showed that plugs B and C were very uniform with respect to CT densities, showing that the samples were homogeneous and without bedding features. The dry and brine-saturated CT densities were 1095±22 and 1570±28 Houndsfield Units (H.U.) for plug B compared to 1136±22 and 1577±24 for plug C. Although the mineralogy of the two plugs is almost identical, the porosity of plug B is higher than that of plug C, which accounts for the lower CT densities for plug B compared to that of plug C.

Imbibition Process--During the imbibition process, brine appeared at the surface boundaries of plug B at low rotational speeds even though the sample was wrapped with Teflon tape. The brine saturation was also higher within the plug near the outermost plug face (with respect to the centrifuge axis of rotation). This is shown in Fig. 6A which is the CT image from the 200 RPM scan. Substantial changes in brine saturation occurred during the 300 RPM speed. The brine distribution after 48 hr at 300 RPM is shown on the 300 RPM scan image on figure 6B. Figure 6B shows that the movement of brine into the plug was in the form of a bank that spread toward the innermost face of the plug (top of images correspond to plug faces closest to the center of the centrifuge). The variations in saturation across horizontal segments of the plug appear uniform by CT images except at the plug edges. The vertical variation on the 300 RPM image shows piston-like displacement of oil and the region of the high oil saturation falls in series with the region of high water saturation. Scan images after higher rotational speeds showed the progression of the water piston toward the innermost plug face. The CT image from the 800 RPM scan indicated that the plug was uniformly saturated with brine. Images from scans taken after periods at higher rotational speeds were similar to the 800 RPM scan, suggesting that only minor additional changes in saturations occurred at speeds from 1,000 to 1,500 RPM.

Very little brine was imbibed at the outer edges of plug C for rotational speeds at or below 200 RPM, except at the outermost face of the plug, as shown in fig. 6C. Fig. 6D shows that significant imbibition occurred after rotation at 300 RPM. The figure shows the parabolic shape of the water distribution along a central plane through the plug. The transition from the region of high brine saturation to the region of high oil saturation in Fig. 6D for plug C is gradual. At higher rotational speeds, the front progressed toward the innermost plug face. After rotation at 800 RPM, the saturation throughout the plug appeared uniform and did not change significantly after rotation at 1,000 and 1,500 RPM.

Similarities among Fig. 6 and Fig. 3 imbibition results can readily be seen. The two figures should be compared qualitatively rather than quantitatively as the grey scales on the images were not calibrated identically to saturations.

Drainage Process--The drainage process was also piston-like for plug B with the oil piston moving from the innermost face toward the outermost plug face with subsequent exposure to higher rotational speeds. Figs. 7A and 7B show CT images from scans after rotation at 400 and 800 RPM speeds. The edge saturation effects that occurred during the imbibition process did not occur during the drainage process from plug B. The plug appeared to be uniformly saturated after the 800 RPM speed, except for the outermost face as shown by Fig. 7B.

The variation in brine saturation changed gradually throughout plug C during the drainage process, as shown in Figs.7C and 7D. Significant changes in saturation for plug C occurred at speeds to 800 RPM. Uniform minor changes in saturations were noted from images taken after exposure to higher rotational speeds.

DISCUSSION

Hysteresis in drainage capillary pressure-saturation curves from tests in which multiple drainage and imbibition saturation cycles were performed did not appear to be consistent with any particular trend. The dominant trend in imbibition capillary pressure hysteresis was a shift of subsequent imbibition curves in the direction of lower brine saturation with more gentle curvature at low capillary pressures and convergence with previous curves at high brine saturations, as shown in Fig. 4. This may be caused by changes in oil trapping with subsequent drainage/imbibition cycles. Wettability indices from subsequent imbibition/drainage cycles in this investigation were reduced, suggesting a decrease in water-wet characteristics with subsequent drainage/imbibition cycles. Trapping of the non-wetting phase is probably responsible to a greater degree than changes in wettability for the reduction in wettability index.

Hassler-Brunner and Rajan capillary pressure-saturation and wettability index results were similar in each case except for plug A. Rajan's model provided more consistent results. The use of more than one model is preferred to ensure that data interpretation is correct (Ruth and Wong, 1990). Capillary pressure results for these high-permeability samples did not appear to change significantly when time at each rotational speed was increased from 1 to 48 hr. Low-permeability samples may be affected differently, however. Wettability indices for sample A were affected significantly by the maximum capillary pressure imposed on the sample during the drainage cycles, whereas sample B appeared to be unaffected. The narrow distribution of pore sizes and high median pore diameter for sample A probably rendered the sample more susceptible to trapping of the non-wetting phase compared to the other two samples.

Wrapping the plugs in Teflon tape did not eliminate edge saturation effects for the high-permeability sample, as shown by the CT scan images. Non-uniform saturation distributions resulted during centrifuge capillary pressure tests at capillary pressures intermediate between the end point saturation conditions.

In designing a centrifuge capillary pressure test for a core sample, it is important to obtain sufficient measurements to describe the shape of the capillary pressure/saturation curves in the regions of high curvature.

Because of the many experimental factors which influence centrifuge capillary pressure results, it is important to record various aspects of fluid compositions, rock characteristics, core preparation, and test conditions along with the centrifuge capillary pressure data to facilitate data analysis and to provide information for resolving discrepancies among experimental results. Table 4 presents a sample form for this purpose. The table was adapted after a similar one by Sprunt (1990).

CONCLUSIONS

1. For these three samples, the order of increasing permeability (C, B, A) was the same as the order of increasing median pore throat diameter.

2. Hysteresis was evident in each multiple-cycle centrifuge capillary pressure experiment. The primary effect of cycle dependent hysteresis for these samples was a reduction in the wettability index with successive drainage and imbibition cycles.

3. Maximum capillary pressures induced during centrifuge capillary pressure tests should be limited to values similar to those occurring in the dynamic displacement process in order to yield representative capillary pressure/saturation and wettability information.

4. CT images showed that fluid distributions during the drainage and imbibition processes were different for plugs B and C. These differences are primarily attributed to pore throat size characteristics.

5. The saturation distributions from CT images of plugs B and C were not uniform until after a certain rotational speed (capillary pressure) was exceeded. Saturation distributions thereafter appeared uniform and were close to residual saturation conditions.

6. Jacketing high-permeability plug B with Teflon tape did not resolve the problem of brine imbibition around the plug margins.

7. Hassler-Brunner and Rajan capillary pressure-saturation and wettability index results were similar in each case, but Rajan's model provided more consistent results. The use of more than one model is preferred to ensure that data interpretation is correct.

ACKNOWLEDGMENTS

The authors extend their appreciation to Ron Masias for conducting many of the centrifuge experiments and Alan Brinkmeyer, both of NIPER, for their assistance in the CT work. We would also like to thank Tom Burchfield, Min Tham, Mike Madden, and Bill Linville for thier suggestions to improve this manuscript. We would like also to acknowledge JAPEX for sponsoring Shogo Suzuki's contribution to this work. This work was sponsored in part by the U.S. Department of Energy under Cooperative Agreement DE-FC22-83FE60149.

REFERENCES

Anderson, W., 1987, Wettability Literature Survey - Part 4: The Effects of Wettability on Capillary Pressure, *Journal of Petroleum Technology*, October, p. 1283-1300.

Anderson, W., 1987, Wettability Literature Survey-Part 5: The Effects of Wettability on Relative Permeability, *Journal of Petroleum Technology,* November, p. 1453-1468.

Batycky, J., McCaffery, F., Hodgins, P. and Fisher, D., 1981, Interpreting Relative Permeability and Wettability From Unsteady-State Displacement Measurements, *Society of Petroleum Engineers Journal,* June, p. 296-308.

Donaldson, E. and Lorenz, P., 1969, Wettability Determination and Its Effect on Recovery Efficiency. *Society of Petroleum Engineers Journal,* March, p. 13-20.

Evrenos, A. and Comer, I., 1969, Numerical Simulation of Hysteretic Flow in Porous Media, paper SPE 2693 prepared for the 44th Annual Fall Meeting of the Society of Petroleum Engineers of AIME, Denver, September 28-October 1.

Hassler, G. and Brunner, E.:, 1945, Measurement of Capillary Pressures in Small Core Samples, *Transactions of AIME*, v. 6, p. 114-123.

Hawkins, J, and Bouchard, A., 1989, Reservoir Engineering Implications of Capillary Pressure and Relative Permeability Hysteresis, paper 8909 presented at the SCA Conference.

Longeron, D., Argaud, M., and Feraud, J., 1986, Effect of Overburden Pressure, Nature, and Microscopic Distribution of the Fluids on Electrical Properties of Rock Samples, paper SPE 15383 prepared for

presentation at the 61st Annual Technical Conference and Exhibition of the Society of Petroleum Engineers, New Orleans, La, October 5-8.

Morrow, N, and Harris, C., 1965, Capillary Equilibrium in Porous Materials, *Society of Petroleum Engineers Journal*, March, p. 15-24.

Rajan, R., 1986, Theoretically Correct Analytical Solution for Calculating Capillary Pressure-Saturation From Centrifuge Experiments, paper J presented at the SPWLA 27th Annual Logging Symposium, June.

Ruth, D., and Wong, S., 1990, Centrifuge Capillary Pressure Curves, Journal of Canadian Petroleum Technology, May-June, Vol. 29, No. 3, p. 67-72.

Sanyal, S., Ramey Jr., H., and Marsden Jr., S., 1973, The Effect of Temperature on Capillary Pressure Properties of Rocks, *in* proceedings of the SPWLA Fourteenth Annual Logging Symposium, May 6-9.

Shaw, J., Churcher, P. and Hawkins, B., 1989, The Effects of Firing on Berea Sandstone, paper SPE 18463 presented at the SPE International Symposium on Oilfield Chemistry, Houston, TX, February.

Sinnokrot, A, Ramey Jr., H., and Marsden, S., 1971, Effect of Temperature Level Upon Capillary Pressure Curves, *Society of Petroleum Engineers Journal*, March, p. 13-22.

Sprunt, E., 1990, Proposed Electrical Resistivity Report Form, *The Log Analyst*, March-April, p. 89-93.

Szabo, M., 1970, New Methods for Measuring the Imbibition Capillary Pressure and Electrical Resistivity Curves by Centrifuge, paper SPE 3038 prepared for the 45th Annual Fall Meeting of the Society of Petroleum Engineers, Houston, TX, Oct. 4-7.

Worthington, A., 1978, A Technique for Detecting Incomplete Saturation of Cores, *Journal of Petroleum Technology*, December, p. 1716-1717.

TABLE 1. - Characteristics of Fired Sandstone Samples Used for Hg Intrusion Porosimetry

Characteristic	Sample A (Bentheimer)	B (Berea)	C (Berea)
Air Permeability, md	3500.0	1330.0	832.0
Porosity, %	26.4	26.0	24.0
Total pore area, m^2/g	3.440	3.314	3.458
Median pore diameter, μm	28.6239	22.2750	16.8361
Avg. pore diameter, μm	0.1497	0.1817	0.1463

TABLE 2. - Characteristics of the Brine and Oil Used in Centrifuge Capillary Pressure and Imbibition Tests

	7 pH brine	10.7 pH brine	oil	7 pH brine and oil	10.7 pH brine and oil
Viscosity, cP	1.01	1.01	1.1	—	—
Density, g/cm^3	1.005	1.005	0.739	—	—
IFT, mN/m	—	—	—	37	31

TABLE 3. - Wettability Indices Calculated From Hassler-Brunner and Rajan Centrifuge Capillary Pressure Results

Sample	Test	Wettability Indices	
		Hassler-Brunner	Rajan
	High RPM, Long Term		
A	1st imb., 2nd drain.	-0.7	-0.1 (0.5)*
A	2nd imb., 3rd drain.	-0.9	0.0 (0.4)*
B	1st imb., 2nd drain.	0.7	0.8
B	2nd imb., 3rd drain.	0.6	0.3
	Low RPM, Long and Short Term		
B	1st imb., 2nd drain. (long term)	0.8	0.8
B	2nd imb., 3rd drain. (short term)	-0.1	0.2
C	1st imb., 2nd drain. (long term)	0.5	0.4
C	2nd imb., 3rd drain. (short term)	-0.1	0.1
	Low RPM, Short Term		
A	1st imb., 2nd drain.	–	1.3
B	1st imb., 2nd drain.	–	0.5
C	1st imb., 2nd drain.	–	0.2

* Based on data for capillary pressures below 6 psi.

Table 4. - Centrifuge Capillary Pressure Report Form

I. Fluid system: oil-gas___ water-oil ___ water-gas___

II. Fluid characterization:

A. Brine

Composition

Cations	Anions	
Na___	Cl___	pH___
K___	SO_4___	density, g/cm^3___
Ca___	HCO_3___	
Mg___	others:___	

Viscosity @ test temperature, cP ___

B. Oil

Oil type: refined oil___ dead oil___ Live oil___

Composition

asphaltenes, % ___
saturates, % ___
polars, % ___
aromatics , % ___

GOR, cm^3/cm^3 ___
Density, g/cm^3 ___
Viscosity, cP ___

C. Gas characteristics:

Composition: nitrogen___ helium___ other___

Viscosity, cP ___
Density, g/cm^3 ___

III. Rock characteristics: plug ID___ depth___length & diameter___

porosity %, before test___ after test___
grain volume, cm^3 ___ method___
pore volume, cm^3 ___ method___
bulk volume, cm^3 ___ method___
k, md: before test___ after test___ method___
confining pressure___

IV. Plug preparation:

state of preservation ___
plugging/trimming fluid ___
cleaning solvents ___
cleaning method ___
cleaning temperature ___
drying temperature ___ humidity___
saturation method used ___
sleeve mat. (if used) ___

Description of marks for consistent orientation ___

V. Centrifuge characteristics:

centrifuge type, model	____	
bucket tilt angle	____	° from horizontal plane
rotor radius, imb.	____	
rotor radius, drain.	____	
axis deviation	____	

VI. Centrifuge test conditions:

confining pressure	____
fluid pressure	____
temperature	____

VII. Centrifuge test data (repeat as necessary for additional drain./imb. cycles):

Cycle No.	____
fluid phase displaced	____
initial saturation volumes	____

target RPM	actual RPM	displaced fluid volume	stabilization time

VIII. Model used for capillary pressure-saturation solution:_____

IX. Method used for wettability calculations:____

X. Capillary pressure-saturation and wettability results (attach tables, graphs, printouts)

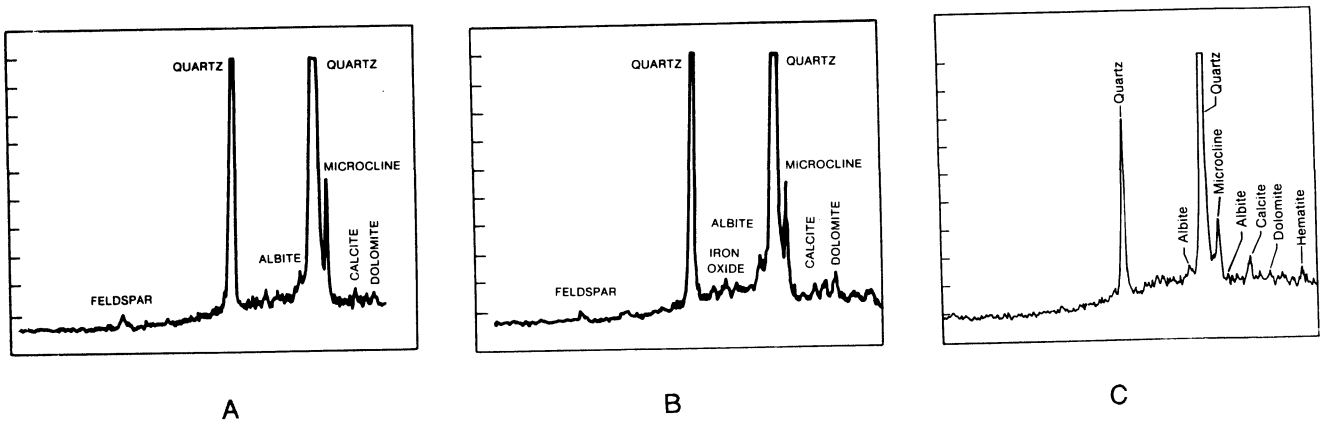

Figure 1. - XRD clay analysis results (recorder scale versus time) for samples A, B, and C showing similarities in mineralogy.

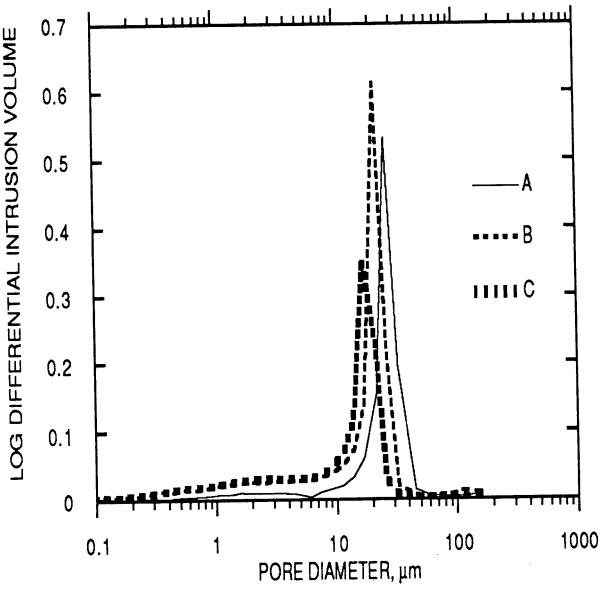

Figure 2. - Mercury injection porosimetry results for samples A, B, and C.

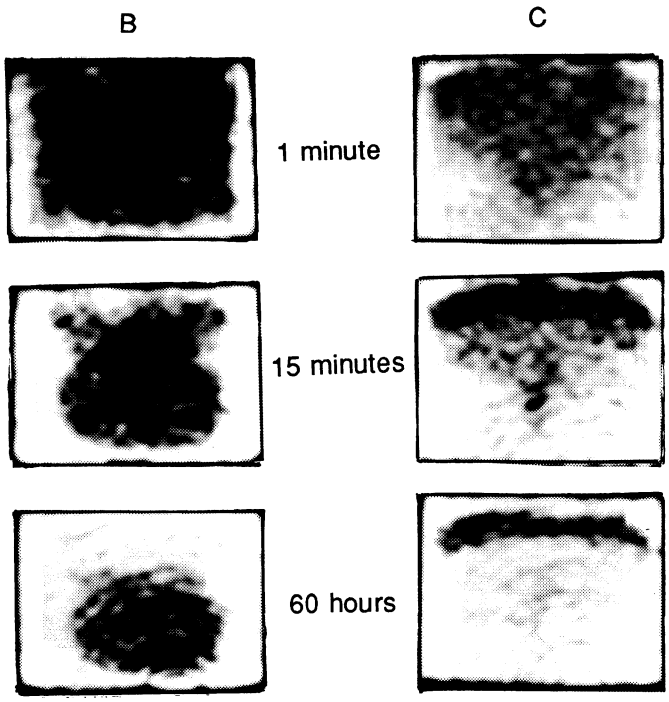

Figure 3. - CT images of plugs B and C as they imbibe brine (light) and displace oil (dark) during static immersion tests.

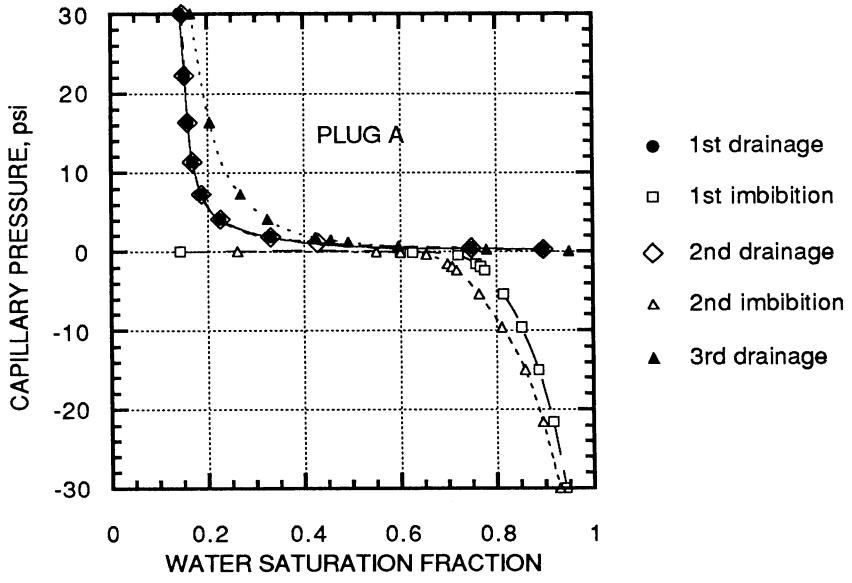

Figure 4. - Capillary pressure results for plug A from high RPM, long-term centrifuge tests.

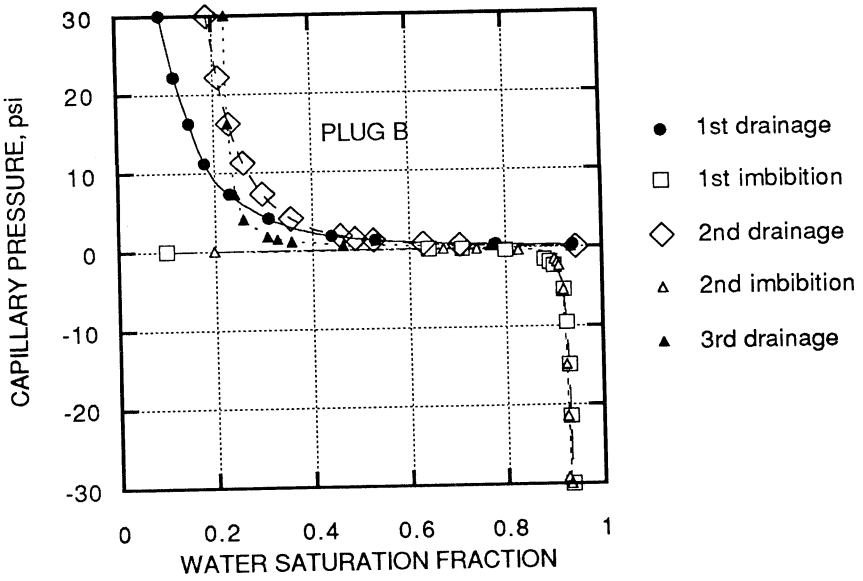

Figure 5. - Capillary pressure results for plug B from high RPM, long-term centrifuge tests.

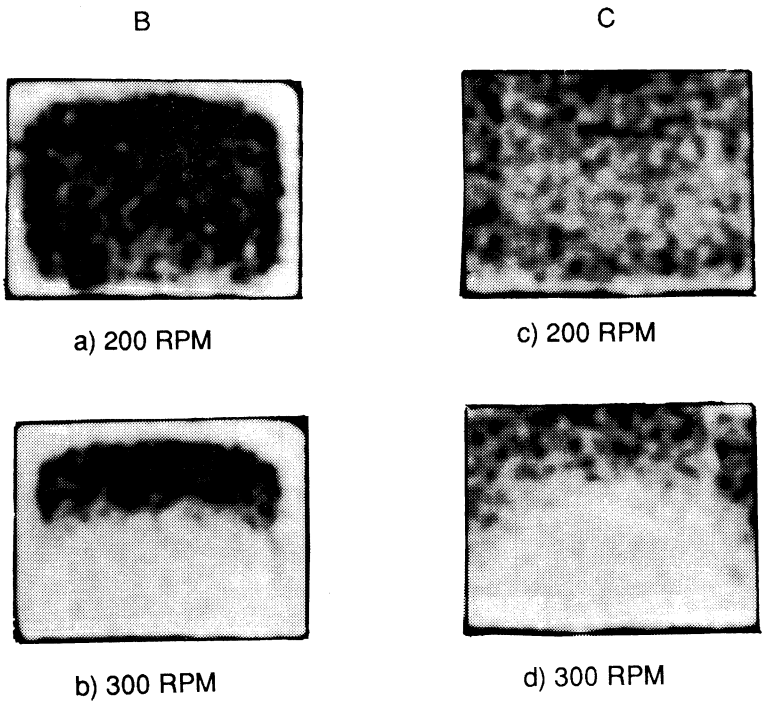

Figure 6. - CT images of plugs B and C after rotation at 200 RPM and 300 RPM during the 1st imbibition cycle showing brine (light) and oil (dark) distributions.

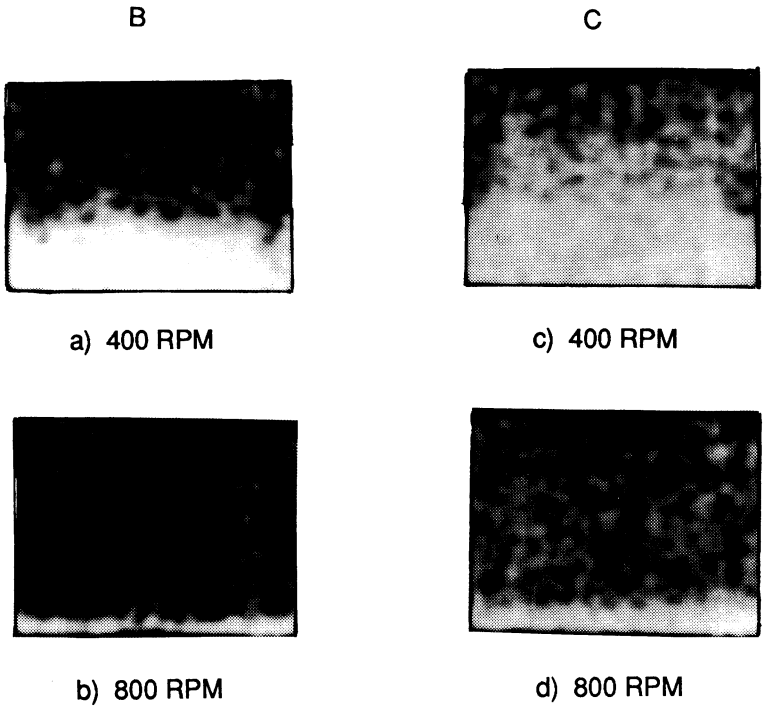

Figure 7. - CT images of plugs B and C after rotation at 400 and 800 RPM during the 2nd imbibition cycle showing brine (light) and oil (dark) distributions.